IEEE Access
Multidisciplinary ⋮ Rapid Review ⋮ Open Access Journal

Received January 25, 2022, accepted February 13, 2022, date of publication February 17, 2022, date of current version February 28, 2022.

Digital Object Identifier 10.1109/ACCESS.2022.3152532

Low-Cost Circularly Polarized Millimeter-Wave Antenna Using 3D Additive Manufacturing

YAZAN AL-ALEM[1], (Senior Member, IEEE), SYED M. SIFAT[2], (Graduate Student Member, IEEE), YAHIA M. M. ANTAR[1,3], (Life Fellow, IEEE), AHMED A. KISHK[2], (Life Fellow, IEEE), ALOIS P. FREUNDORFER[3], (Senior Member, IEEE), AND GAOZHI XIAO[4], (Fellow, IEEE)

[1]Department of Electrical and Computer Engineering, Royal Military College of Canada, Kingston, ON K7K 7B4, Canada
[2]Department of Electrical and Computer Engineering, Concordia University, Montreal, QC H3G 1M8, Canada
[3]Department of Electrical and Computer Engineering, Queen's University, Kingston, ON K7L 3N6, Canada
[4]Advanced Electronics and Photonics, National Research Council, Ottawa, ON K1A 0R6, Canada

Corresponding author: Yazan Al-Alem (yazan.al-alem@rmc-cmr.ca)

This work was supported by the High Throughput and Secure Networks (HTSN) Challenge Program at the National Research Council Canada.

ABSTRACT An efficient single-layer printed feed is used with a low-cost 3D printed polarizer. The feed is made on a single substrate layer. The proposed antenna gain is 15 dBi, and the overlapped impedance-axial ratio bandwidth is 20%. The proposed structure is a low-cost structure that can be fabricated in any modest fabrication facility. The feed does not require any plated vias, which tremendously simplifies the fabrication process and lowers the cost. The feed is very well suited for integration with integrated circuit transceiver systems. The proposed structure does not require any feeding network design. Hence, it relaxes the design process and avoids the losses associated with such feeding network. The proposed element can be employed in an array configuration with adequately suppressed side lobes. The element cost, simplicity, and gain performance are superior to other proposed solutions in the literature.

INDEX TERMS Additive manufacturing, circular polarization, high gain antennas, low-cost antennas.

I. INTRODUCTION

In many long-range wireless communication applications, signals are communicated through a wireless line of sight propagating electromagnetic wave. The transmitting and receiving antennas are designed to have adequate directivity to focus and capture the electromagnetic energy within the line of sight. Since these antennas communicate mainly through the line of sight as contrary to fading wide coverage channels, the transmitting and receiving antennas alignment is critical to prevent any polarization mismatch. Circularly polarized antennas are superior to linearly polarized antennas for these scenarios. Incident Right-Handed Circularly Polarized (RHCP) waves are scattered from surfaces in the form of Left-Handed Circularly Polarized (LHCP) waves, and vice versa. Such a feature of circular polarization is advantageous in long-range wireless microwave links, where the non-line of sight signals (usually the strongest component is reflected from the ground) are seen as cross-polarization waves by the receiving antenna. Thus, it eliminates any possibility of fading and destructive interference with the line of sight waves. In satellite communication systems, due to the considerable distance between the low orbit satellite and the earth antennas, it is tough to have a perfect alignment between the communicating antennas. In addition, the different atmospheric layers and the weather conditions can have a significant effect on the propagating wave polarization. Therefore, using circularly polarized antennas has a tremendous advantage in eliminating the need for polarization alignment, hence preventing any polarization mismatch losses [1], [2]. Many exciting ideas were proposed in various structures to realize circular polarization. In [3]–[5], Substrate Integrated Waveguide (SIW) and Printed Ridge Gap Waveguide (PRGW) were used as feeds. Such feeds are suitable for mm-wave applications due to their packaged nature. However, they require a relatively large number of vias and are considered multi-layer structures, therefore increasing their fabrication complexity. In [6]–[8],

The associate editor coordinating the review of this manuscript and approving it for publication was Debdeep Sarkar.

a polarizer was used with an open-ended waveguide feed. Open-ended waveguide feeds have a superior impedance bandwidth performance. However, they are very bulky and unsuitable for integration with an Integrated Circuit (IC) transceiver solution. An open-ended waveguide feed requires a special transition to connect it to a transmitter or receiver circuitry, usually through a coaxial feed. In [9], a printed solution was proposed. Such a solution uses multi-layer PCB technology and requires plated vias, increasing the cost and complexity of fabrication. In [5], a differentially fed antenna solution was proposed. It used multiple PCB layers, the array gain achieved was 13.5 dBi, and the axial ratio bandwidth was 10%, not to mention the complexity of the design due to incorporating a differential feed layer. In [10], a polarizer was used with a linear array of patch antennas, and multiple-layers were used to have a stacked 8 element antenna array configuration of stacked patches to widen the impedance bandwidth. However, the antenna array had an axial ratio bandwidth of 11.7% and a gain of 13 dBi. The Microstrip Line slot feeding the patch antenna generates high back lobe radiation at millimeter-wave frequencies, not to mention the associated loss in the feeding network. In [11], an end-fire log-periodic antenna pointed to the boresight was fed using an SIW feeding network. Such structure has a considerable fabrication complexity. Here, we focus on designing a low-cost structure that can be fabricated in any modest fabrication facility. The structure uses a single-layer feed using printed technology. The feed doesn't require any plated vias, which tremendously simplifies the fabrication process and lowers the cost. The feed is a linearly polarized antenna that utilizes radiation from open stubs to boost the boresight directivity. The antenna polarization is converted to a circular polarization using a 3D printed polarizer. The polarizer material is RGD840 thermoplastics with dielectric constant 3 and loss tangent 0.01. The polarizer adequately transforms the polarization of the antenna to a circular polarization while at the same time it further boosts the gain. 3D Additive Manufacturing is an emerging technology that has a promising potential in providing high flexibility and reduced fabrication cost. The technique allows the construction of 3D objects from a digital 3D model, giving flexibility and freedom in defining the model geometry using CAD software and maintaining a low fabrication cost. The proposed structure uses a simplified, low-cost feed with a single substrate (Rogers 5880), which is advantageous. The feed is very well suited for integration with integrated circuit transceiver systems. The proposed structure does not require any feeding network design. Hence, it relaxes the design process and avoids any losses associated with such feeding network. The proposed structure has a wideband impedance bandwidth of 20%. The proposed antenna gain is 15-dBi, and the Axial Ratio bandwidth is 30%. The overlapped Axial Ratio-Impedance bandwidth is 20%. The proposed element can be employed in an array configuration with adequately suppressed side lobes.

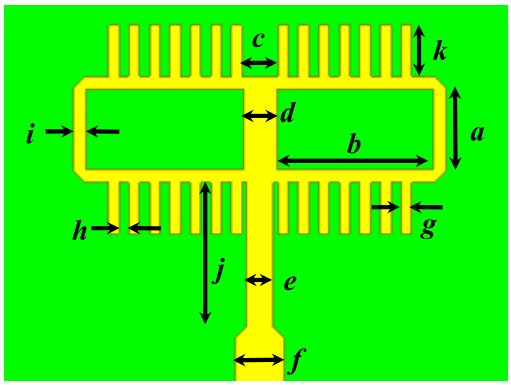

FIGURE 1. Proposed printed feed antenna.

TABLE 1. Dimensions (millimeters) of the proposed antenna in Fig. 1.

a	*b*	*c*	*d*	*e*	*f*
3.9	7.645	1.77	1.66	1.3	2.4
g	*h*	*i*	*j*	*k*	
0.5	0.5	0.625	7	2.475	

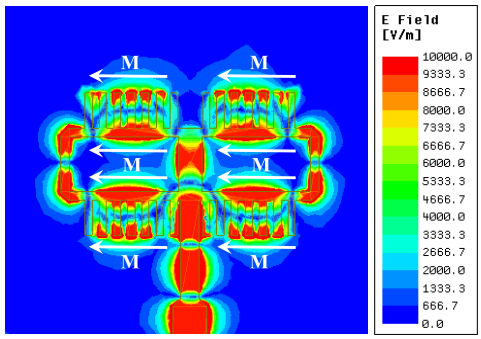

FIGURE 2. Electric field heat map of the proposed antenna in Fig. 1.

II. PROPOSED PRINTED FEED

Fig. 1 shows the proposed antenna printed feed. The substrate used is Rogers 5880, with a dielectric constant of 2.2, loss tangent of 0.0009, and 0.787 mm thickness. The proposed antenna utilizes the fringing fields from the open-ended microstrip line stubs. These fringing fields can be represented equivalently as magnetic currents. By increasing the number of stubs, a significant electrical aperture area can be obtained and can produce significant directivity in the boresight. Further details about the radiation mechanism can be found in [12]–[15].

In this work, two elements are combined with a single feed point, the number of stubs can be increased to add more resonances within the operating bandwidth, which can increase the impedance matching bandwidth to 20 %. Table 1 lists the dimensions of the proposed structure. Fig. 2 shows the electric field heat map. As can be seen, the fringing fields can have a significant aperture area and equivalently can be represented as magnetic currents. It is also important to note that since the upper and lower stubs are laid in opposite directions, they have to maintain 180° phase shift feed to keep boresight radiation. The antenna loop can be designed with such property along the dimension *a*. Loading

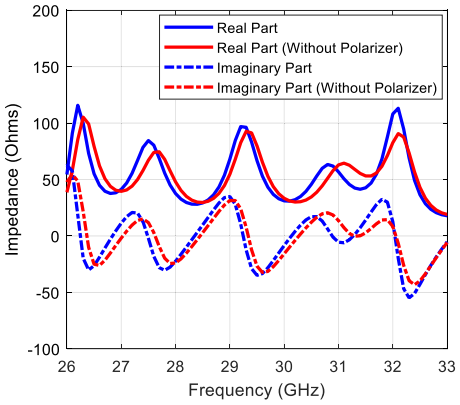

FIGURE 3. Input impedance of the proposed antenna.

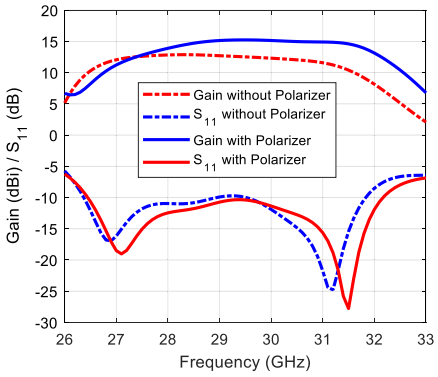

FIGURE 4. Gain and S_{11} of the proposed antenna.

the loop with the stubs enhances the phase shift balance between the upper and lower stubs over a wide bandwidth. This can be observed from the electric field heat map in Fig. 2 by noting that there are almost two guided wavelengths for the microstrip line loop. The first is in the region loaded by stubs, where the guided wavelength is larger than the second region, which is not connected to any stubs. Fig. 3 shows the input impedance with multiple resonances within the desired operating bandwidth. Fig. 4 shows the gain and reflection coefficient of the proposed antenna, a 20% 10-dB return loss matching bandwidth is achieved with a peak directivity of 12 dBi.

III. DIELECTRIC POLARIZER

Electromagnetic polarizers are well covered in the literature, specifically in optics [16], [17]. The operation mechanism of these polarizers depends on the 45°-plane wave incident on the dielectric slab. Fig. 5 shows the Floquet-port unit cell analysis configuration. Master and slave boundary conditions are applied along the x and y directions. An incident plane wave with an angle of 45° is generated at the port underneath the dielectric slab. This plane wave can be decomposed into two orthogonal modes (Transverse Electric, TE, and Transverse Magnetic, TM). In this case, the propagating TE and TM waves experience a different effective dielectric constant due to the filling ratio difference. By changing the filling ratio and height a 90° phase shift between the TE

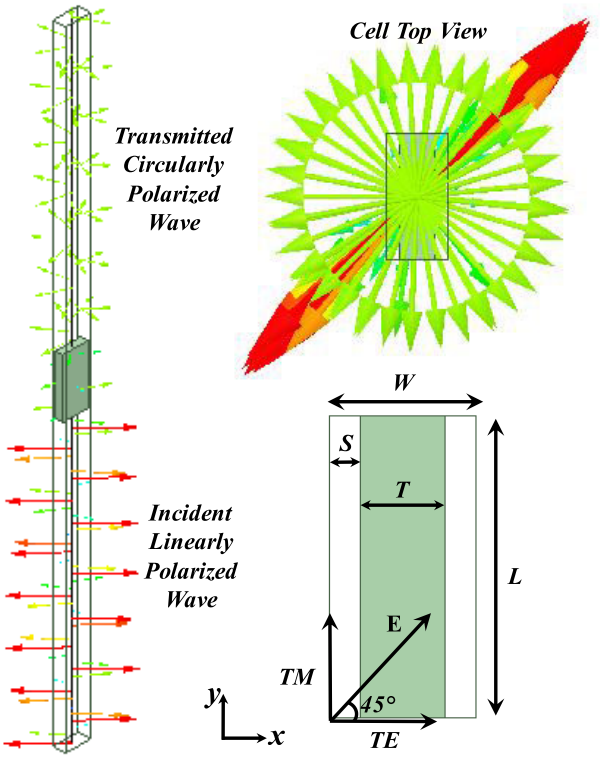

FIGURE 5. Proposed dielectric polarizer unit cell analysis.

and TM wave can be obtained. Hence, the total propagating wave beyond the dielectric slab becomes circularly polarized. In [18], an asymptotic relation for the effective dielectric constant for each polarization was presented. This relation is valid for thin substrates with a low filling ratio. Here, the filling ratio is 0.57. Therefore, a numerical solver is used to set the dielectric slab dimensions. The asymptotic approximations for the effective dielectric constants for the TE (i.e. along the x-axis), and the TM (i.e. along the y-axis) modes are given in (1-2), the phase shift between the TM and TE waves can be calculated according to (3). Despite the fact that these equations are valid for low filling ratio, they are still very handy in giving an excellent initial set of dimensions for the numerical solver. It is also worth noting that the periodic boundary conditions represent an infinite structure and study only the case of normal plane wave incidence. These conditions are different from the finite polarizer conditions excited by the proposed antenna. Nonetheless, this analysis is crucial in getting an initial set of parameters to design the finite polarizer structure.

$$\varepsilon_{eff\_x} \approx 1 \tag{1}$$

$$\varepsilon_{eff\_y} \approx 1 + (\varepsilon_r - 1)\frac{T}{W} \tag{2}$$

$$\Delta\theta = \frac{2\pi f}{c}\left(\sqrt{\varepsilon_{eff\_y}} - 1\right)H \tag{3}$$

Dielectric polarizers are very attractive at higher frequencies, as their sizes become smaller, especially if a higher dielectric constant is used. They do not require any printed metallic geometries, making them easy to realize. Using 3D

TABLE 2. Dimensions (millimeters) of the dielectric polarizer unit cell in Fig. 5, "*H*" represents the dielectric polarizer height.

W	*S*	*L*	*H*	*T*
2.9	0.62	6	14	1.66

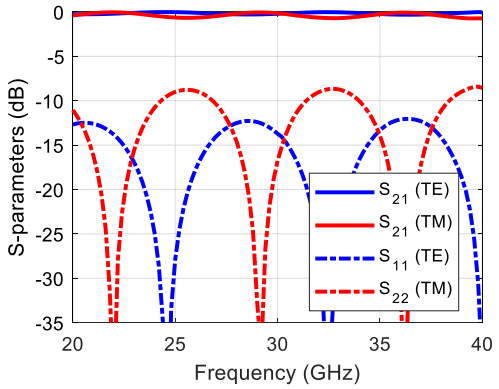

FIGURE 6. Transmission and reflection coefficients of the dielectric polarizer.

printing technology would make it easier and less expensive to manufacture. In [17], it was shown that printing a metallic patch at one side of the polarizer slab can increase the axial ratio bandwidth to 60%. However, in this work, we only use a dielectric slab to ease the fabrication. The polarizer achieved axial ratio bandwidth is 46%, which is broader than the antenna matching impedance bandwidth. Table 2 lists the dimensions of the dielectric slab. RGD840 thermoplastics material with dielectric constant value of 3, and loss tangent, 0.01 is used. Fig. 6 shows the transmission and reflection coefficients of each mode. As can be seen, there are minimal reflection and almost unity transmission coefficients for each mode, indicating almost magnitude equality of TE and TM electric field components. Hence, the axial ratio can be calculated from the angle difference between these modes, as given in (4). Fig. 7 shows the phase difference between the TE and TM modes, which is set to be 90° at the center frequency (i.e., 30 GHz). Fig. 8 shows the corresponding axial ratio covering a 46% bandwidth.

$$AR = \left| 20 \log_{10} \left| \tan\left(\frac{\Delta\theta}{2}\right) \right| \right| \tag{4}$$

IV. PROPOSED CIRCULARLY POLARIZED ANTENNA STRUCTURE

Fig. 9 shows the proposed circularly polarized antenna structure. The dielectric polarizer is co-designed with the antenna feed. As can be seen, the antenna feed is fully printed and requires no vias, and hence it is very simple and easy to fabricate. Copper fully backs the feed; therefore, it reduces back lobe radiation and improves the front-to-back ratio. The dielectric polarizer dimensions were optimized to boost the gain further and maintain a wide axial ratio bandwidth. Fig. 4 shows the S_{11} and gain of the proposed structure with the polarizer. As can be seen, the

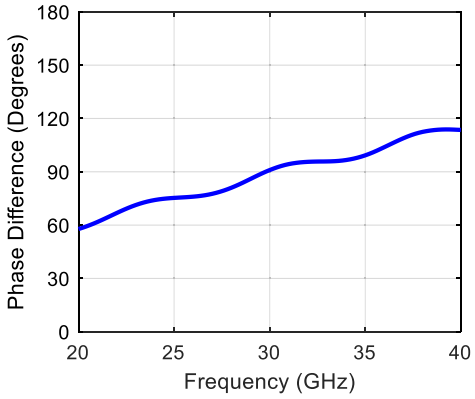

FIGURE 7. Phase difference between transmitted TE and TM components.

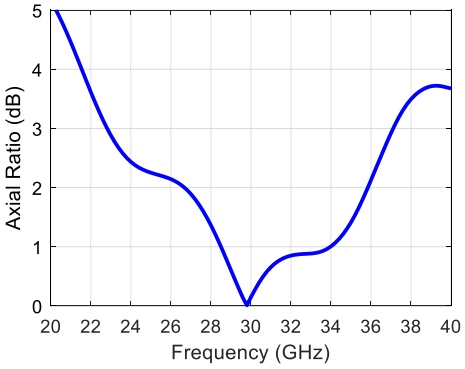

FIGURE 8. Dielectric polarizer axial ratio.

TABLE 3. Dimensions (millimeters) of the proposed antenna in Fig. 9.

A	*B*	*C*	*D*	*E*	*F*	*G*	*H*
24.525	36.34	2.818	5.128	7.17	15.6	16	22
I	*J*	*K*	*L*	*M*	*N*	*O*	*P*
0.53	2.12	1.98	1.075	4.263	32.3	12.3	1.4

reflection coefficient is minimally perturbed with the use of a polarizer, as the polarizer is designed to be fully transparent (i.e., the transmission coefficient of the polarizer is almost 0 dB). Hence, it appears transparent to the antenna and has minimal effect on its input impedance. This is a considerable relaxation for the design process. As shown in Fig. 4, the gain goes up to 15 dBi with good stability over the operating bandwidth (Note: dBiC unit can be used instead of dBi to indicate CP gain as well). As observed, the polarizer improves the gain of the feed by 3 dB. Table 3 lists the dimensions of the proposed structure in Fig. 9. Fig. 10 shows the axial ratio without a polarizer indicating a linear polarization. Fig. 11 shows the axial ratio when the polarizer is used. A 30% axial ratio bandwidth is achieved.

V. ANTENNA ARRAY CONFIGURATION

The proposed element in the previous section is electrically large ($2.2\lambda_o$), which raises the question of whether the element can be further expanded in a larger linear array without generating grating lobes? The answer is yes, where the high directivity of the element factor suppresses the grating lobes in the array factor. Hence, by performing pattern

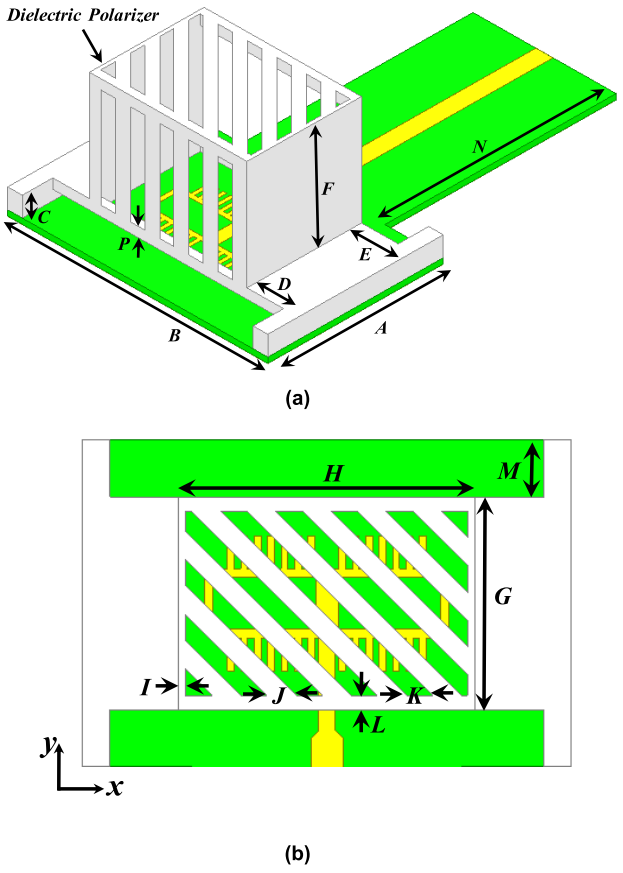

FIGURE 9. Proposed circularly polarized antenna, (a) isometric view, and (b) top view.

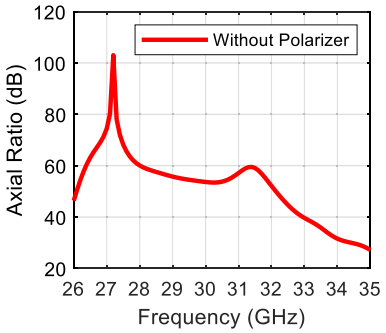

FIGURE 10. Axial ratio of the proposed antenna without using a polarizer.

multiplication, the resultant pattern grating lobes would be adequately suppressed. Fig. 12 shows a linear array made of two elements, the center to center distance between the elements is 34.3 mm ($3.43\lambda_o$). Fig. 11 shows the axial ratio of the array configuration. As can be seen the array axial ratio is minimally perturbed once it is compared with the single element. Fig. 13 shows that the gain of the two elements proposed array goes up to 18 dBi. Also as can be seen from Fig. 13, the mutual coupling between the elements is less than -30 dB. This would significantly relax the array design process. As shown in Fig. 14, the side-lobes of the array are well suppressed.

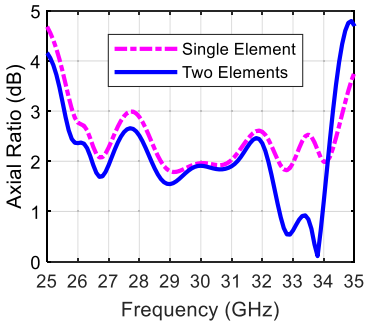

FIGURE 11. Axial ratio of the proposed antenna using a polarizer.

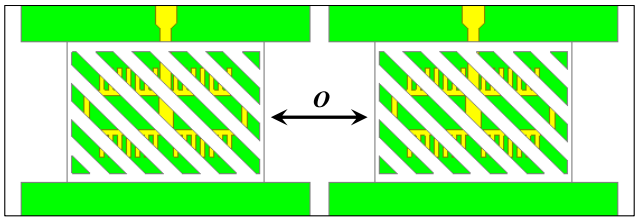

FIGURE 12. Two-element antenna array configuration.

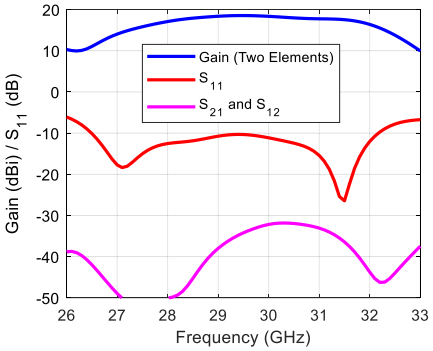

FIGURE 13. Gain and S-parameters of the two-element antenna array.

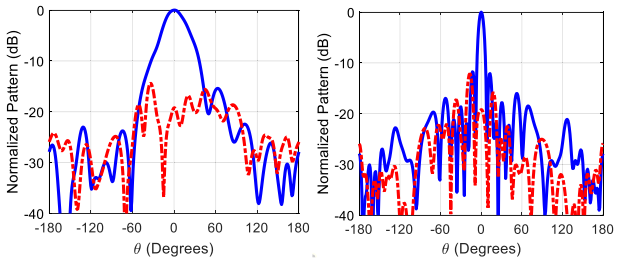

FIGURE 14. Radiation patterns of the proposed circularly polarized antenna, left (*yz*-plane), right (*xz*-plane), solid (RHCP/co-polar), and dotted (LHCP/cross-polar), at 30 GHz.

VI. PROTOTYPING RESULTS

Fig. 15 shows the fabricated prototype. Fig. 16 shows the measured radiation patterns of the proposed antenna in *xz* and *yz* planes. As can be seen, the side-lobes are well-suppressed. It is important to note that the long feed line exists only for characterization purposes to keep it far enough from the end-launch connector. In an integrated circuit board, the transceiver IC can be connected directly to the antenna microstrip line edge through a bonding wire. In such case the extra loss and any distortion by the elongated line and the bulky end launch connector are eliminated. Also the height

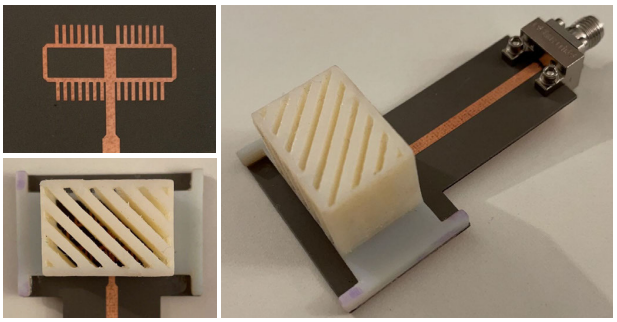

FIGURE 15. Fabricated prototype.

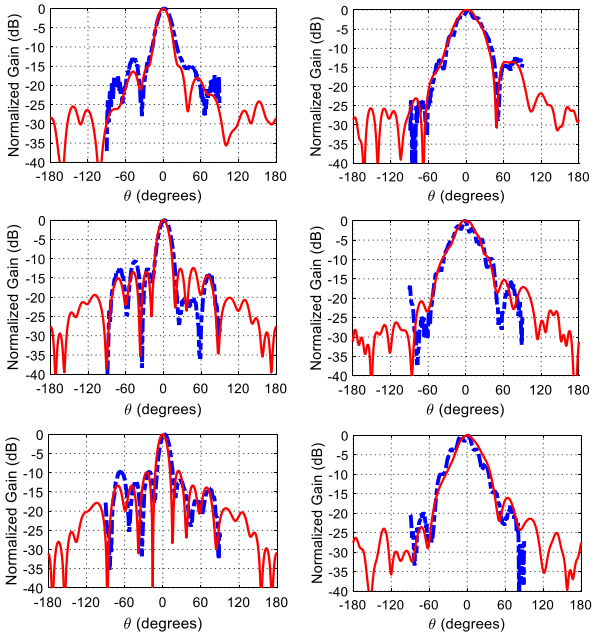

FIGURE 16. Radiation patterns of the proposed (RHCP) circularly polarized antenna, *xz*-plane (left), and *yz*-plane (right), at 28, 30, and 31 GHz from top to bottom, measured (dotted), and simulated (solid).

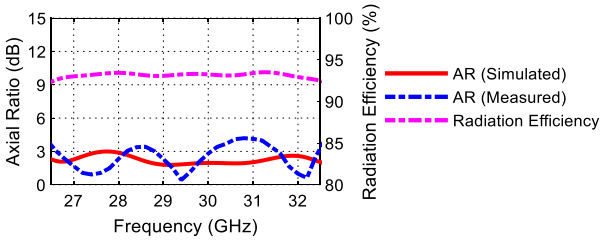

FIGURE 17. Measured axial ratio and calculated radiation efficiency.

of the polarizer is 14 mm, a lower polarizer height can be made with a higher dielectric constant material (A higher dielectric constant material with mm-wave characterization was not available for use in our fabrication facility). Thus a dielectric constant of 3 was used. Fig. 17 shows the measured axial ratio, as can be observed there is a slight deviation of the axial ratio at 31 GHz (i.e. 4.1 dB), which could be due to some possible miss-alignment of the antenna, and tolerances in the material and the fabrication process. However, the axial ratio is still within an acceptable range for such low-cost prototyping. Fig. 18 shows that the measured gain goes up

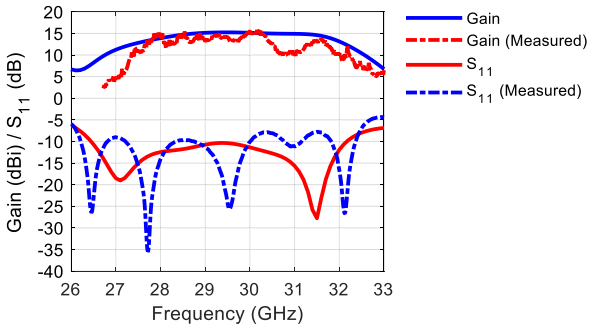

FIGURE 18. Measured gain and S_{11}.

TABLE 4. Comparison with other works.

Work	Gain (dBi)	Bandwidth (%)	Technology (Feeding)	Frequency (GHz)
[10]	13	11.7	8 Elements Stacked Patches	30
[5]	13.5	10	PRGW Differential Fed	30
[9]	12.3	22.5	2x2 EBG Spiral	38
[19]	11.45	29.3	Fabry-Perot ME-Dipole	14
[20]	11.5	19	2x2 EBG Patches	26
[21]	14.6	16.7	SIW Differential Feed	60
Present	15	20	Printed Single Layer	30

to 15 dBi, and the 10 dB return loss bandwidth is 20 %. Thus a reasonably acceptable agreement with simulated results is achieved. The simulated efficiency is shown in Fig. 17, it goes up to 93 % as expected due to the simplified feed design. It is worth noting that the microstrip line width is 2.4 mm, a tapered transition is needed to connect it to the end lunch connector, such tapering along with the end lunch connector transition can cause some perturbation for the S_{11} response, nonetheless it is still within an acceptable range with a return loss value less than 10 dB all over the operating bandwidth. Table 4 compares the proposed antenna performance metrics with other works in the literature. As can be noticed, the proposed antenna has the merit of simplicity (via-less) with high gain, and acceptable bandwidth performance.

VII. CONCLUSION AND FUTURE WORK

A novel single-layer printed feed has been used with a low-cost 3D printed polarizer. The feed has been made on a single substrate. The proposed antenna has achieved 15 dBi gain and 20% bandwidth. Future work will investigate the employment of the element in a more extensive array.

REFERENCES

[1] D. Liu, B. Gaucher, U. Pfeiffer, and J. Grzyb, *Advanced Millimeter-Wave Technologies*. Chichester, U.K.: Wiley, 2009.
[2] C. A. Balanis, *Antenna Theory Analysis and Design*, 3rd ed. Hoboken, NJ, USA: Wiley, 2005.
[3] Y. Li and K.-M. Luk, "A 60-GHz wideband circularly polarized aperture-coupled magneto-electric dipole antenna array," *IEEE Trans. Antennas Propag.*, vol. 64, no. 4, pp. 1325–1333, Apr. 2016, doi: 10.1109/TAP.2016.2537390.
[4] L. Zhang, K. Wu, S.-W. Wong, Y. He, P. Chu, W. Li, K. X. Wang, and S. Gao, "Wideband high-efficiency circularly polarized SIW-fed S-dipole array for millimeter-wave applications," *IEEE Trans. Antennas Propag.*, vol. 68, no. 3, pp. 2422–2427, Mar. 2020, doi: 10.1109/TAP.2019.2940468.

[5] M. M. M. Ali and A. Sebak, "Printed RGW circularly polarized differential feeding antenna array for 5G communications," *IEEE Trans. Antennas Propag.*, vol. 67, no. 5, pp. 3151–3160, May 2019, doi: 10.1109/TAP.2019.2900411.
[6] K. X. Wang and H. Wong, "A wideband millimeter-wave circularly polarized antenna with 3-D printed polarizer," *IEEE Trans. Antennas Propag.*, vol. 65, no. 3, pp. 1038–1046, Mar. 2017, doi: 10.1109/TAP.2016.2647693.
[7] K. X. Wang and H. Wong, "A wideband CP antenna by using 3D printing polarizer," in *Proc. IEEE Int. Conf. Comput. Electromagn. (ICCEM)*, Feb. 2016, pp. 180–182, doi: 10.1109/COMPEM.2016.7588573.
[8] K. X. Wang and H. Wong, "Design of a wideband circularly polarized millimeter-wave antenna with an extended hemispherical lens," *IEEE Trans. Antennas Propag.*, vol. 66, no. 8, pp. 4303–4308, Aug. 2018, doi: 10.1109/TAP.2018.2841414.
[9] E. Baghernia, M. M. M. Ali, and A. R. Sebak, "2 × 2 slot spiral cavity-backed antenna array fed by printed gap waveguide," *IEEE Access*, vol. 8, pp. 170609–170617, 2020, doi: 10.1109/ACCESS.2020.3024564.
[10] M. Akbari, M. Farahani, A. R. Sebak, and T. A. Denidni, "Ka-band linear to circular polarization converter based on multilayer slab with broadband performance," *IEEE Access*, vol. 5, pp. 17927–17937, 2017, doi: 10.1109/ACCESS.2017.2746800.
[11] Y.-X. Zhang, Y.-C. Jiao, and L. Zhang, "Wideband circularly polarized array antennas with sequential-rotation polarization grid and simplified full-SIW feeding networks," *IEEE Trans. Antennas Propag.*, vol. 68, no. 8, pp. 6088–6097, Aug. 2020, doi: 10.1109/TAP.2020.2985065.
[12] Y. Al-Alem and A. A. Kishk, "Highly efficient unpackaged 60 GHz planar antenna array," *IEEE Access*, vol. 7, pp. 19033–19040, 2019, doi: 10.1109/ACCESS.2019.2895904.
[13] Y. Al-Alem and A. A. Kishk, "Efficient millimeter-wave antenna based on the exploitation of microstrip line discontinuity radiation," *IEEE Trans. Antennas Propag.*, vol. 66, no. 6, pp. 2844–2852, Jun. 2018, doi: 10.1109/TAP.2018.2823865.
[14] Y. Al-Alem and A. A. Kishk, "Low-cost high-gain superstrate antenna array for 5G applications," *IEEE Antennas Wireless Propag. Lett.*, vol. 19, no. 11, pp. 1920–1923, Nov. 2020, doi: 10.1109/LAWP.2020.2974455.
[15] Y. Al-Alem, S. M. Sifat, Y. M. M. Antar, A. A. Kishk, and G. Xiao, "Low-cost circularly polarized millimeter-wave antenna using 3D additive manufacturing dielectric polarizer," in *Proc. IEEE Int. Symp. Antennas Propag. USNC-URSI Radio Sci. Meeting (APS/URSI)*, Dec. 2021, pp. 1–2.
[16] M. Mutlu, A. E. Akosman, and E. Ozbay, "Broadband circular polarizer based on high-contrast gratings," *Opt. Lett.*, vol. 37, no. 11, p. 2094, Jun. 2012, doi: 10.1364/OL.37.002094.
[17] J. Wang, Z. Shen, W. Wu, and K. Feng, "Wideband circular polarizer based on dielectric gratings with periodic parallel strips," *Opt. Exp.*, vol. 23, no. 10, p. 12533, May 2015, doi: 10.1364/OE.23.012533.
[18] J. D. Shumpert, "Modeling of periodic dielectric structures (electromagnetic crystals)," Ph.D. dissertation, Univ. Michigan, Ann Arbor, MI, USA, 2001. [Online]. Available: http://citeseerx.ist.psu.edu/viewdoc/download;jsessionid=7D9BBD283DBF37ECDC06F0308B68BCA1?doi=10.1.1.402.4513&rep=rep1&type=pdf
[19] W. Cao, X. Lv, Q. Wang, Y. Zhao, and X. Yang, "Wideband circularly polarized Fabry–Pérot resonator antenna in Ku-band," *IEEE Antennas Wireless Propag. Lett.*, vol. 18, no. 4, pp. 586–590, Apr. 2019, doi: 10.1109/LAWP.2019.2896940.
[20] C. Ma, Z.-H. Ma, and X. Zhang, "Millimeter-wave circularly polarized array antenna using substrate-integrated gap waveguide sequentially rotating phase feed," *IEEE Antennas Wireless Propag. Lett.*, vol. 18, no. 6, pp. 1124–1128, Jun. 2019, doi: 10.1109/LAWP.2019.2910657.
[21] D. J. Bisharat, S. Liao, and Q. Xue, "High gain and low cost differentially fed circularly polarized planar aperture antenna for broadband millimeter-wave applications," *IEEE Trans. Antennas Propag.*, vol. 64, no. 1, pp. 33–42, Jan. 2016, doi: 10.1109/TAP.2015.2499750.

YAZAN AL-ALEM (Senior Member, IEEE) received the B.Sc. degree in electrical engineering from the University of Jordan, Amman, Jordan, in 2010, the M.Sc. degree in electrical engineering from the American University of Sharjah, Sharjah, United Arab Emirates, in 2015, and the Ph.D. degree from Concordia University, Montreal, QC, Canada, in 2019. He was a recipient of the Concordia University International Tuition Award of Excellence and the American University of Sharjah Full Graduate Teaching and Research Assistantship.

SYED M. SIFAT (Graduate Student Member, IEEE) received the B.Sc. degree in electrical and electronic engineering from American International University–Bangladesh (AIUB), Dhaka, Bangladesh, in 2013, and the M.Sc. degree in electrical and computer engineering from Concordia University, Montreal, QC, Canada, in 2019, where he is currently pursuing the Ph.D. degree in electrical engineering. Since 2017, he has been working as a Research Assistant at Concordia University. Before his master's degree, he worked at City Group of Industries Ltd., Narayanganj, Bangladesh, and GSL Export Ltd., Chittagong, Bangladesh, as a Project Engineer. His research interests include designing millimeter-wave (mm-wave) antennas, microwave reciprocal/nonreciprocal design and analysis, RF amplifiers, active and passive microwave components, metamaterials, guiding structures, and electromagnetic bandgap (EBG) structures. He received the Concordia University International Tuition Award of Excellence for his outstanding academic record.

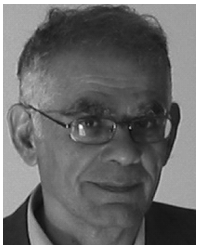

YAHIA M. M. ANTAR (Life Fellow, IEEE) received the B.Sc. degree (Hons.) in electrical engineering from Alexandria University, Alexandria, Egypt, in 1966, and the M.Sc. and Ph.D. degrees in electrical engineering from the University of Manitoba, Winnipeg, MB, Canada, in 1971 and 1975, respectively. In May 1979, he joined the Division of Electrical Engineering, National Research Council of Canada, Ottawa, ON, Canada. In November 1987, he joined the Department of Electrical and Computer Engineering, Royal Military College of Canada, Kingston, ON, where he has been a Professor, since 1990. He has authored or coauthored over 200 journal articles, several books, and chapters in books, over 450 refereed conference papers, holds several patents, has chaired several national and international conferences, and has given plenary talks at many conferences. He was appointed as a member of the Canadian Defense Advisory Board (DAB) of the Canadian Department of National Defense, in January 2011. He is a fellow of the Engineering Institute of Canada (FEIC) and the Electromagnetic Academy. He is also an International Union of Radio Science (URSI) Fellow. In 1977, he held a Government of Canada Visiting Fellowship at the Communications Research Center, Ottawa. In 2003, he was awarded the Royal Military College of Canada "Excellence in Research" Prize and the RMCC Class of 1965 Teaching Excellence Award in 2012. In October 2012, he received the Queen's Diamond Jubilee Medal from the Governor-General of Canada in recognition of his contribution to Canada. He was a recipient of the 2014 IEEE Canada RA Fessenden Silver Medal for Ground Breaking Contributions to Electromagnetics and Communications and the 2015 IEEE Canada J. M. Ham Outstanding Engineering Education Award. In May 2015, he received the Royal Military College of Canada Cowan Prize for excellence in research. He was also a recipient of the IEEE-AP-S of the Chen-To-Tai Distinguished Educator Award in 2017. He has supervised and co-supervised over 90 Ph.D. and M.Sc. theses at the Royal Military College and at Queen's University, several of which have received the Governor-General of Canada Gold Medal Award, the Outstanding Ph.D. Thesis of the Division of Applied Science, as well as many best paper awards in major international symposia. He served as the Chair for Canadian National Commission (CNC), URSI, from 1999 to 2008, Commission B, from 1993 to 1999, and has a cross-appointment at Queen's University, Kingston. In May 2002, he was awarded the Tier 1 Canada Research Chair in electromagnetic engineering which has been renewed in 2016. He was elected by the URSI to the Board as the Vice President, in August 2008 and 2014, and to the IEEE Antennas and Propagation (AP-S) AdCom. In 2019, he was elected as the 2020 President-Elect for IEEE AP-S, and will serve as its President, in 2021. He has served as an Associate Editor for many IEEE and IET journals and an IEEE-APS Distinguished Lecturer.

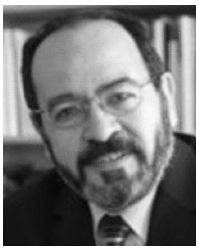

AHMED A. KISHK (Life Fellow, IEEE) received the Ph.D. degree from the University of Manitoba, Winnipeg, MB, Canada, in 1986. In 1986, he joined the University of Mississippi, Oxford, MS, USA, first as an Assistant Professor and then a Professor. Since 2011, he has been a Professor with Concordia University, Montreal, QC, Canada, as the Tier 1 Canada Research Chair in Advanced Antenna Systems. He has authored or coauthored more than 340 refereed journal articles and 450 conference papers. He is the coauthor of four books and several book chapters, and the editor of three books. His research interests include millimeter wave antennas, beamforming networks, dielectric resonator antennas, microstrip antennas, and EBG. He is a fellow of Electromagnetic Academy, and a fellow of the Applied Computational Electromagnetics Society (ACES). He won the 1995 and 2006 outstanding paper awards for the Applied Computational Electromagnetic Society Journal. He was a recipient of the 1997 Outstanding Engineering Educator Award from Memphis Section of the IEEE, the Outstanding Engineering Faculty Member of the Year in 1998 and 2009, the Faculty Research Award for outstanding performance in research in 2001 and 2005, the Award of Distinguished Technical Communication for the entry of *IEEE Antennas and Propagation Magazine*, in 2001, the Valued Contribution Award for outstanding Invited Presentation from the Applied Computational Electromagnetic Society, the Microwave Theory and Techniques Society, Microwave Prize, and the 2004 and 2013 Chen-To Tai Distinguished Educator Award of the IEEE Antennas and Propagation Society. During 2013–2015, he was a Distinguished Lecturer with the Antennas and Propagation Society. During 1993–2014, he was the Editor of the *IEEE Antennas and Propagation Magazine*. From 1998 to 2001, he was the Editor-in-Chief of the ACES Journal. He was a guest editor of the special issue on artificial magnetic conductors, soft/hard surfaces, and other complex surfaces, in the IEEE TRANSACTIONS ON ANTENNAS AND PROPAGATION, in 2005. He was the 2017 AP-S President.

ALOIS P. FREUNDORFER (Senior Member, IEEE) received the B.A.Sc., M.A.Sc., and Ph.D. degrees from the University of Toronto, Toronto, ON, Canada, in 1981, 1983, and 1989, respectively. In 1990, he joined the Department of Electrical Engineering, Queen's University, Kingston, ON, Canada. Since 1990, he has been involved in the nonlinear optics of organic crystals, coherent optical network analysis, and microwave integrated circuits. He was involved in high-speed IC design for use in lightwave systems with bit rates in excess of 40 Gb/s and in millimeter wave integrated circuits used in wireless communications. His current research interests include growing 3-D low-temperature ceramics on ICs and printed circuit boards with applications to sensors and low power tunable circuits.

GAOZHI (GEORGE) XIAO (Fellow, IEEE) received the Ph.D. degree from Loughborough University, U.K., in 1995. He is currently a Principal Research Officer of the National Research Council. Canada. He is also the Editor-in-Chief of the IEEE JOURNAL OF RADIO FREQUENCY IDENTIFICATION and an Associate Editor-in-Chief of the IEEE TRANSACTIONS ON INSTRUMENTATION AND MEASUREMENT. He has managed large research and development projects in industries, academics, and government labs, covering areas, including RFID/NFC, flexible/printable/wearable electronics, fiber optic sensor systems, photonic sensing and measurement, structural health monitoring, indoor air quality monitoring, structural materials, and smart materials. He has brought several technologies from concepts to products.